Published in final edited form as:

J Med Genet. 2022 November ; 59(11): 1044–1057. doi:10.1136/jmedgenet-2021-108115.

Complete loss of the X-linked gene CASK causes severe cerebellar degeneration

Paras A Patel[1,2], **Julia Hegert**[5], **Ingrid Cristian**[5], **Alicia Kerr**[2,3], **Leslie EW LaConte**[2,6], **Michael A Fox**[3,4], **Sarika Srivastava**[2,7], **Konark Mukherjee**[2,8,*]

[1]Translational Biology, Medicine, and Health Graduate Program, Fralin Biomedical Research Institute, Roanoke, VA 24016, USA

[2]Center for Neurobiology Research, Fralin Biomedical Research Institute, Roanoke, VA 24016, USA

[3]Virginia Tech, Department of Biological Sciences, Blacksburg, VA 24060, USA

[4]Virginia Tech, School of Neuroscience, Blacksburg, VA, 24060, USA

[5]Orlando Health, APH, MP 331, USA

[6]Virginia Tech Carilion School of Medicine, Department of Basic Science Education, Roanoke, VA 24016, USA.

[7]Department of Internal Medicine, Virginia Tech Carilion School of Medicine, Roanoke, VA 24016, USA.

[8]Department of Psychiatry, Virginia Tech Carilion School of Medicine, Roanoke, VA 24016, USA.

Abstract

Background: Heterozygous loss of X-linked genes like CASK and MeCP2 (Rett syndrome) causes developmental delay in girls, while in boys loss of the only allele of these genes leads to epileptic encephalopathy. The mechanism for these disorders remains unknown. CASK-linked cerebellar hypoplasia is presumed to result from defects in Tbr1-reelin-mediated neuronal migration.

Method: Here we report clinical and histopathological analyses of a deceased 2-month-old boy with a CASK-null mutation. We next generated a mouse line where CASK is completely deleted (hemizygous and homozygous) from post-migratory neurons in the cerebellum.

*Corresponding Author, Konark Mukherjee, FBRI, 2 Riverside Cir., Roanoke, VA 24014, Fax: 540-985-3373, Telephone: 540-526-2035, konark@vtc.vt.edu.

Author contribution:

Experiments were conceived by KM, PP, MF, IC. Data analyzed by KM, MF, PP, JH, LL, SS. Experiments conducted by PP, AK, JH. Paper written by KM, PP, MF, LL, SS, IC, JH. All authors read and approved the final manuscript.

Competing Interests:

The authors have declared that no conflict of interest exists.

Declarations:

Ethics Approval and Consent to Participate:

All studies described herein were approved by the Virginia Tech Institutional Animal Care and Use Committee and Virginia Tech Institutional Review Board.

Result: The CASK-null human brain was smaller in size but exhibited normal lamination without defective neuronal differentiation, migration, or axonal guidance. The hypoplastic cerebellum instead displayed astrogliosis and microgliosis, markers for neuronal loss. We therefore hypothesize that CASK loss-induced cerebellar hypoplasia is the result of early neurodegeneration. Data from the murine model confirmed that in CASK loss, a small cerebellum results from post-developmental degeneration of cerebellar granule neurons. Further, at least in the cerebellum, functional loss from CASK deletion is secondary to degeneration of granule cells and not due to an acute molecular functional loss of CASK. Intriguingly, female mice with heterozygous deletion of CASK in the cerebellum do not display neurodegeneration.

Conclusion: We suggest that X-linked neurodevelopmental disorders like CASK mutation and Rett syndrome are pathologically neurodegenerative; random X-chromosome inactivation in heterozygous mutant girls, however, results in 50% of cells expressing the functional gene, resulting in a non-progressive pathology, whereas complete loss of the only allele in boys leads to unconstrained degeneration and encephalopathy.

One sentence summary of study:

CASK loss causes cerebellar degeneration.

Keywords

CASK; MICPCH; neurodegeneration; X-linked; X-inactivation; cerebellum; ataxia

Introduction:

Heterozygous mutations in certain X-linked genes (e.g., CDKL5, MeCP2 in Rett syndrome, and CASK in MICPCH (mental retardation and microcephaly with pontine and cerebellar hypoplasia (OMIM: 300749)) are linked to postnatal microcephaly in girls [1]. Hemizygous mutations in these same genes give rise to progressive epileptic encephalopathy and lethality in boys [2–4]. Rett syndrome was the first such disorder to be reported; it was described as a cerebral atrophic syndrome by Andreas Rett in 1966 [5]. Until the 1990s, Rett syndrome was considered a neurodegenerative disorder [6]. With the discovery, however, of the MeCP2 gene association, postmortem autopsy observations, and the development of preclinical models, focus shifted to dendritic morphology and synapse development and dysfunction, resulting in the reclassification of Rett syndrome as a neurodevelopmental disorder [7] [8]. Studies of the cellular pathology associated with MeCP2 loss in boys with epileptic encephalopathies have, however, been limited [9].

MICPCH is also considered a neurodevelopmental disorder that occurs due to heterozygous mutations in the X-linked gene CASK (calcium/calmodulin-dependent serine protein kinase) in girls. Despite the microcephaly associated with CASK mutation being described as postnatal and progressive, females with MICPCH grow into adulthood, often with intellectual disability that is non-progressive [10–14]. Such mutations in hemizygous males are, however, lethal. These boys exhibit epileptic encephalopathy with pronounced cerebellar hypoplasia and progressive supratentorial atrophy [4 15 16]. Regression of motor skills has also been noted in a girl with MICPCH in adolescence [17]. The cellular

pathology of CASK-linked disorders remains uncertain. This problem is exacerbated by the fact that CASK-null mice die within hours of birth and do not exhibit a difference in brain size or morphology from their wild type littermates at birth [18]. Based on the standard Theiler developmental staging of mice [19], the immediate postnatal period of mice best parallels the third trimester of human fetal development (Carnegie staging; [20]), making any interpretation of postnatal brain pathology difficult.

Although often considered to be a component of presynaptic terminals, CASK in fact is ubiquitously expressed in the body [21 22] and has been implicated in a variety of functions outside the brain, including cell polarization [23], renal development, and cardiac conductivity [24 25]·[26 27]. CASK is proposed to be involved in axonal branching [28], dendritic arborization [29], dendrite spinogenesis [30], and synaptogenesis [31]. Thus, many hypotheses as to why loss of CASK leads to defects in brain development can be proposed. CASK null mice, however, fail to exhibit any defects in synaptogenesis or neuronal morphology. The only detectable phenotype is a change in action potential-independent neurotransmission [18].

CASK also has a function in regulating gene transcription [32–34]. It has been suggested that CASK translocates to the nucleus, where it regulates the function of T-box transcription factor (Tbr-1) [34 35]. It is proposed that CASK forms a ternary complex with CINAP (CASK-interacting nucleosome assembly protein) and Tbr-1 to induce expression of molecules such as reelin that play a crucial role in brain development [33]. Reelin is a secreted extracellular molecule critical for neuronal migration [36]. Indeed, both in the reeler mice and Tbr-1 knockout mice, defects in proper lamination of cortex are seen [37 38]. In addition to the cortex defects, reeler mice also display a hypoplastic disorganized cerebellum with defects in neuronal migration and suppressed neurogenesis [37]. The neurodevelopmental function of CASK has been specifically attributed to CASK's interaction with Tbr-1 and its presumed regulation of reelin expression [13 39 40]. Although the molecular role of CASK has been attributed to Tbr-1 binding or synaptic function, Tbr-1 null mice themselves show no difference in size of other brain regions including the cortex and cerebellum other than a smaller olfactory bulb [38]. Further, complete abrogation of the CASK-Tbr1 interaction fails to induce any structural defect in the brain or cerebellum [41]. Similarly, abolishing synaptic function does not seem to affect brain development in embryonic mice or brain structure in postnatal mice [42 43]. Thus it is unlikely that these purported functions of CASK can account for the changes seen in MICPCH. Using a murine model, we previously demonstrated that the histopathology of cerebellar hypoplasia in MICPCH involves a reduction in the number of cells in the internal granular layer (IGL) [44]. This could either be due to changes in the development of granule cells or the loss of granule cells after formation (degeneration), as seen in the weaver mouse [45].

Here, we report a detailed clinical description and autopsy findings from a 2-month-old boy harboring the CASK null mutation R27* (R27Ter). Although the brain is small, the clear presence of tertiary gyri that form near term, as well as proper cortical and cerebellar lamination, argue against defects in neuronal migration; instead, we uncover evidence of neuronal damage and loss (degeneration) suggested by reactive astrogliosis and microgliosis in the cerebellum. We then design and execute a genetic experiment in mice

that provides conclusive evidence that loss of CASK indeed produces neurodegeneration (loss of developed neurons) in the cerebellum. Most pontocerebellar hypoplasias (PCH) are progressive, but based on the postnatal brain growth pattern, it has been hypothesized that MICPCH has a distinct pathogenic mechanism [46]. We instead provide evidence that mechanistically, MICPCH in girls with heterozygous CASK mutations is also degenerative, and the non-progressive course of MICPCH is dictated by the unique X-linked inheritance pattern in which 50% of brain cells express the normal gene.

Materials and Methods:

Statement of Ethics

All studies described herein were approved by the Virginia Tech Institutional Animal Care and Use Committee and Institutional Review Board.

Statistics

A two-tailed Student's t-test was used when comparing two genotypes in each experiment to compute significance with an alpha of 0.05.

Clinical History, EKG (Supplemental Figure 1) and EEG spectral analysis method

Please see Supplemental file.

Generation of Mouse Lines

Calb2-Cre mice (strain 010774) were obtained from Jackson Laboratory, *Cask*^{floxed} mice (strain 006382) were a kind gift from Prof. Thomas Südhof. *Cask*^{floxed} females were bred with *Calb2*-Cre positive males to generate the F1 cross *Cask*^{floxed}::*Calb2*-Cre. F1 mice were bred to Ai14-LSL-tdTomato-positive males obtained from Jackson Laboratory (strain 007914) to generate fluorescent reporter mice. F1 mice were genotyped by PCR using primers targeted at either LoxP elements, a sequence within the Cre gene, or a sequence within the tdTomato gene. All lines were from a C57BL/6J background backcrossed for at least 25 generations.

Antibodies and Material Reagents

Bassoon monoclonal antibodies were obtained from Enzo Lifescience, GFAP (glial fibrillary acidic protein) monoclonal antibodies were obtained from Invitrogen, calbindin (D28K) polyclonal antibody from Invitrogen, synaptophysin, NeuN and S100β antibodies were obtained from Sigma and Iba1 antibody was obtained from FUJIFILM Wako. Secondary antibodies conjugated with AlexaFluor 488, 550 and 633 were obtained from Thermofisher. Hardset Vectashield™ with DAPI was obtained from Vector Laboratories.

Immunostaining of Mouse Tissue

For all immunostaining, mice were sacrificed by trans-cardiac perfusion first with phosphate buffered saline (PBS) for exsanguination and subsequently with 4% paraformaldehyde for fixation of tissues. Brains were dissected and post-fixed for at least 24 hours in 4% paraformaldehyde. After post-fixation, brains were hemisected along the longitudinal

fissure and 50μm sagittal sections were cut using a ThermoScientific™ Microm HM650V Vibratome. Sections were submerged in permeabilization/blocking solution composed of 10% fetal bovine serum and 1% Triton-X 100 in PBS overnight at +4°C.

Rabbit anti-calbindin was diluted at 1:50 in blocking solution and mouse anti-bassoon was diluted at 1:200 in blocking solution. Rabbit anti-NeuN antibody was diluted at 1:50. For glial immunostaining, mouse anti-GFAP was diluted at 1:200 in blocking solution and mouse anti-S100B was diluted at 1:1000. After blocking/permeabilization overnight, free-floating sections were incubated for 3 hours in dilute primary antibody at room temperature. After incubation in primary antibody, sections were washed 3 times for 5 minutes in PBS before being incubated in secondary antibody for the respective host species for 1 hour at room temperature. Sections were again washed and mounted on slides using VECTASHIELD® anti-fade medium. Synapse quantification was performed using the automated SynQuant algorithm [47].

Immunostaining of Human Tissue

Human tissue obtained during autopsy was post-fixed in 10% formalin overnight, embedded in paraffin, and subsequently sectioned into 20μm sections onto charged slides. Slides were deparaffinized with 3 changes of poly-xylenes for 10 minutes each time and rehydrated using an ethanol gradient from 100%−95%−70%−50%-H_2O for 5 minutes in each condition. Antigen retrieval was conducted by boiling slides in 10mM sodium citrate buffer with 0.1% Tween-20 for 10 minutes in a domestic microwave followed by running the slides under cold tap water for 10 minutes. Immunostaining for GFAP, calbindin, synaptophysin, S100B, and Iba1 (rabbit polyclonal antibody diluted at 1:500) was then conducted using the same procedure described for mouse tissue. Control tissue was obtained from a female born at 30 post conception weeks and died at 6 PNW.

Motor Behavioral Assays

Accelerating Rotarod experiments were conducted by placing 4 *Cask*$^{(floxed)}$::*Calb2*-Cre mice at P100 (post-ataxia onset), at P48 (pre-ataxia onset), and age-matched *Cask*$^{(floxed)}$ control mice on an accelerating Rotarod, beginning at 2 cycles/minute and accelerating at a rate of 5 cycles/minute until mice fell off the platform. Three trials were conducted in succession for each mouse, with 5 minutes of rest between trials.

Results

Complete CASK loss in humans causes encephalopathy and cerebellar atrophy

MICPCH subjects with heterozygous CASK mutations are known to live past their 30s. *Cask*$^{+/-}$ female mice are fertile beyond 6 months. We have allowed four *Cask*$^{+/-}$ mice to age more than two years (considered to be old for mice). All four mice survived to that age without adverse events. We did not observe any obvious phenotypes in these aged mice compared to wild-type littermates. The cerebellum displayed the typical layers and configuration without severe deterioration, indicating that the disorder is non-progressive (Supplemental Figure 2).

Null mutation of *CASK* in mice is, however, lethal and in boys, produces progressive encephalopathy. Due to the early lethality of *Cask* null mice, the postnatal pathology of complete *Cask* loss has been difficult to study to date. Here we describe detailed clinical findings and autopsy results from a 2-month-old boy with a *CASK* null mutation who expired due to hypoventilation and neurogenic respiratory failure. A copy number variation study was unremarkable, but next generation sequencing of genes revealed a de novo c.79C>T (p.Arginine27Ter) *CASK* mutation in exon 2 (Figure 1A). This *CASK* mutation introduces a stop codon in the very N-terminus of the CASK protein, precluding expression of any splice variant of CASK (Supplemental Figure 3). Magnetic resonance imaging (MRI) indicated normal lateral and third ventricles with an elongated fourth ventricle. The cerebellum appeared markedly hypoplastic with an extremely rudimentary vermis. The small posterior fossa was filled with fluid (Figure 1B). The corpus callosum was thin but present without any midline shift, and myelination was delayed for age. The cavum septum pellucidum seemed to be more prominent. No heterotopic cells were noted in any area, but there was some simplification of gyral pattern, particularly in the frontal cortex. The brain stem appeared to be extremely thin.

Video electroencephalographic (vEEG) monitoring was done both during awake and sleeping states. Awake-state background EEG displayed a burst-suppression pattern with variable amounts of bursts and suppressions (Figure 1F and Supplemental Figure 4). This EEG pattern is typical of Ohtahara syndrome, a devastating epileptic encephalopathy that usually co-occurs with *CASK*-null mutations [4 15 16]. The burst phase was dominated by a mixture of theta and delta waves. Overall, the EEG retained its symmetry in both hemispheres but was discontinuous. No electroclinical seizures were observed during the two hours period of recording, although intermittent and independent sharp waves were observed, predominantly in the right temporal and occipital region. The sleep EEG was similar to the waking EEG and included burst-suppression signals. A spectral analysis of the entire epoch revealed skewing towards lower frequency with delta and alpha power dominating the spectra (Figure 1D, E).

At autopsy, head circumference was 32.7 cm, with a 37.0 cm crown-rump length and crown-heel length of 51.0 cm. The decedent was small for his age, and the brain weight was 300.8 grams, which is 60% of what is expected at this age (Supplemental Figure 5). Except for lung, heart, and spleen, most other organs were smaller than expected but had an overall normal gross appearance (autopsy report). The brain was well formed with normal gyrification in the cerebral hemispheres. Tertiary gyri were present, and there was no evidence of polymicrogyria or other abnormal configuration. The Sylvian fissure was well formed, and the leptomeninges were clear (Figure 2A). Vascularization, including the circle of Willis, was normally formed. The central part of the cerebral hemispheres was edematous, and the septum cavum pellucidum was present (0.9 cm in vertical length). The basal ganglia displayed a normal architecture bilaterally. The left hippocampus was also architecturally normal with a serpiginous appearance. The right hippocampus had a blurred appearance (Supplemental Figure 6 and autopsy report). The thalamus was normally formed and firm. The lateral ventricles were not dilated; the midbrain was very small with a patent but pinpoint cerebral aqueduct, and the fourth ventricle was slit-like. The cerebellum and the pons were markedly hypoplastic (Figure 2A, Supplemental Figure 6). The cerebellum,

despite hypoplasia, had a normal configuration but did not exhibit the usual folia. There was no evidence for heterotopia of cells. Although the cerebellum had grown both laterally and in length, it remained a very thin, leaf-like structure (Figure 2A). The anterior vermis was not identifiable and appeared to be membrane-like; cerebellar hemispheres were thin, flattened and firm (Supplemental Figure 7). The spinal cord was of uniform caliber and had no obvious pathology (autopsy report).

Absence of CASK does not affect neuronal migration, axonal guidance, or lamination in humans but may promote neuronal loss

Histologically, the cerebellum itself displayed proper cellular organization, with a defined external granular layer (EGL), molecular layer, and internal granular layer (IGL). The two-dimensional growth of the cerebellum, which is mediated by the formation of the Purkinje cell plate [48], remained unperturbed as described above, and there was a uniform single layer of developed Purkinje cells between the molecular layer and the internal granular layer. The dendritic arbors of Purkinje cells are clearly visible in the molecular layer (Figure 2B). Overall, the migration of Purkinje cells, which requires reelin [48], is largely unaffected. The R27ter subject's age was 10 postnatal weeks (PNW), and comparisons were made with a cerebellum from a PNW 6 pre-term infant who died of a non-neurological cause around the same date. The migratory pattern of granule cells was visible and appropriate for age in the R27ter cerebellum, but the IGL appears hypocellular (Figure 2B,M and Supplemental Figure 7G,H). The dentate nucleus was absent, and the anterior vermis displayed very few granule cells (Supplemental Figure 7D and 8). Inferior olivary nuclei were poorly formed and did not display pseudohypertrophy. The midbrain consisted of astrocytic cells with pink cytoplasm and some neuronal cells, but no organized substantia nigra was noted (Supplemental Figure 9A). Sections of the cortex indicated orderly and proper neuronal migration; the germinal matrix was appropriately thinned for this age (Supplemental Figure 9B). The white matter tracts were discreet and adequate for the decedent's age (Supplemental Figure 6). The basal ganglia and hippocampi were properly organized and unremarkable. The midbrain and pons displayed corticospinal tracts. The cerebral aqueduct was patent and dilated. Within the pons, the pontine decussation was seen and the locus coeruleus properly formed (Supplemental Figure 9C). The medullary olives were poorly formed, and the fourth ventricle was widely patent. The spinal cord was unremarkable with adequate anterior horn cells and uniform radiating column. The central canal was patent throughout (Supplemental Figure 6 and official autopsy report).

Histologically, almost all organs including the bone marrow, heart, and intestines were unremarkable. The endocrine glands also appeared normal, except for the adrenal cortex, which was thinned out. The kidneys had appropriate and orderly glomerular and tubular development (Supplemental Figure 10C,D).

Data clearly indicate that although CASK loss affects the size of the brain globally, the cerebellum and brainstem are disproportionately affected. Both in murine models and the human subject, early lethality is likely linked with the dysfunction of the brainstem leading to respiratory failure. *Cask* null mice display hypoventilation and die within hours of birth although the brain is of normal size and properly laminated at death [18].

The normal lamination and configuration of the brain in both CASK null humans and mice suggests that the histological pathology related to CASK loss is likely to be degenerative, with neuronal loss. Two common hallmarks of neuronal damage and neuronal loss are loss of synapses and reactive gliosis. We therefore next evaluated the cerebellum of the decedent for evidence of synapses and of gliosis (Figure 2C–J). Previous studies in the murine model have shown that CASK loss-of-function does not negatively impact synapse formation [18 44], and in the human cerebellum evaluated here, immunostaining revealed that levels of the synaptic marker synaptophysin in the decedent's cerebellar cortex were similar to levels observed in a control cerebellum (Figure 2C,E). Strikingly, the synaptophysin staining appeared to be mostly perisomatic for Purkinje cells, although punctae are also clearly visible in dendrites of the molecular layer (ML). This staining pattern is different than would be expected for the age; in typical development, the most prominent synaptophysin staining from 34 weeks onward is in the ML [49]. Early in development, perisomatic synapses are mostly formed by climbing fibers which translocate postnatally to dendrites in the ML [50]. Parallel fibers (the axons of granule cells) also form synapses on Purkinje cell dendrites in the ML. The lack of synaptophysin staining in the ML is most likely attributable to the loss of abundant parallel fibers and incomplete translocation of the climbing fibers in the early postnatal phase. We next examined the cerebellum for the presence of gliosis; GFAP and S100β staining was done for astrocytes and Bergmann glia, and Iba1 staining was done for microglia, the resident immune cells of the brain critical for clearing dead cells and debris which often accumulate in regions of neurodegeneration (Figure 2 C,D) [51]. Data indicate that, compared to the control, the decedent exhibits ~5-fold higher amounts of GFAP immunoreactivity, specifically in the IGL (Figure 2C,F). In fact, large reactive astrocytes in the IGL were readily observed only in the CASK null cerebellum (Supplemental Figure 11). The CASK null brain also exhibited more microglia in the IGL (Figure 2 D,G). Finally we observed increased S100β immunoreactivity both in the ML and the IGL, with an increased number of S100β positive cells (Figure 2D,H-J). Together these data suggest that loss of CASK produces early neurodegenerative changes, causing the CASK-linked phenotype to typically manifest postnatally. Finally, we investigated myelination within the cerebellar cortex using FluoroMyelin lipid staining (Figure 2K) and observed that although the myelination pattern exhibited a disturbed arrangement within the IGL of the 10 PNW R27Ter subject, discrete myelinated tracts were noted, in contrast to the near-absent staining observed in the 6 PNW control subject, indicating progress of myelination with maturity (Figure 2 K,L). The number of cells in the IGL, however, was low (Figure 2M). The histological findings thus indicate that the disorganized white matter may be secondary to ongoing cerebellar grey matter degeneration. In fact, the development and synaptogenesis of the fetal and neonatal cerebellum and its connections in humans are well described [49 52], and our study suggests that this process is not delayed or stalled; instead, the structures that develop earlier, such as the dentate nucleus, are earlier to degenerate. This same trend is seen in the cerebellar cortex, where the vermis, which develops earlier than the cerebellar hemispheres, appears to be highly atrophied and rudimentary [49 52]. Based on our histological observations, we hypothesize that loss of CASK induces cerebellar cortical degeneration, specifically after migration of cerebellar glutamatergic cells such as granule cells or neurons of the dentate nucleus. To test this idea, we next employed murine genetic

experiments, where CASK is deleted in a temporally and spatially specified manner using Cre-LoxP-mediated gene excision.

Calb2-Cre targets post-migratory granule cells and a subset of Purkinje cells in the cerebellum

Previous neuroimaging data and the comprehensive CASK null brain histological autopsy results presented here clearly indicate that within the brain, loss of CASK is likely to disproportionately affect the hindbrain including the brainstem and cerebellum. In particular, CASK-linked lethality most likely results from effects on the brain stem. To avoid any lethality, our focus, therefore, is to evaluate the long-term effect of CASK loss only in the cerebellum. We have previously demonstrated that CASK loss does not affect cerebellar development [44]. In order to test our hypothesis, we needed to disassociate CASK loss from developmental migration of cerebellar neurons. To do so, we chose a mouse line in which Cre-recombinase is driven by an endogenous promoter of the signaling molecule *Calb2* (calretinin/calbindin2), reported earlier [53]. It has been shown that *Calb2* expresses in nearly all granule cells in the cerebellum [54 55], but the exact timing of initiation of *Calb2*-Cre gene recombination in granule cells was not known. There have also been conflicting reports about the expression of *Calb2* in the Purkinje cells within the cerebellum [54 55]. We therefore first tested the recombination specificity of *Calb2*-Cre in mice at ages when the cerebellum is still developing and displays both the EGL and IGL (P8 and P15). We crossed *Calb2*-Cre mice with Cre-recombination indicator mice (LSL-tdTomato) (Figure 3A). The distribution of the tdTomato-expressing neurons serves as a proxy for CASK deletion when *Calb2*-Cre mice are crossed with *Cask*^{floxed} mice in parallel (Figure 3B). Our data indicate that *Calb2*-Cre is active in the cerebellum as early as P8. By P8, recombination was observed in granule cells but only after migration into the IGL; recombination was also observed in many post-migratory Purkinje cells (Figure 3C). By P15, Calb2-Cre already exhibited robust recombination in many parts of the brain and in the entirety of post-migratory granule cells. Dense cellular distribution with recombination was seen in the cerebellum, hippocampus, striatum and olfactory bulb. Sparsely distributed cells were observed throughout the brain, including the cortex (Figure 3D, E). The brainstem displayed minimal recombination, with sparsely tdTomato-labeled cells. Within the cerebellum, all granular cells in the IGL and a subset of post-migratory Purkinje cells were positive for recombination at P15. Cells in the EGL, however, did not display any recombination, indicating that *Calb2*-Cre-driven recombination occurs only after migration of granule cells (Figure 3E). Our data thus indicate that *Calb2*-Cre specifically leads to deletion of CASK both in a subset of Purkinje cells and in granule cells after migration by P15 and is not likely to affect the brainstem or its function. Thus crossing *Calb2*-Cre with *Cask*^{floxed} line generates mice where CASK deletion is naturally synchronized to migration within different cerebellar neurons.

Deletion of CASK from cerebellar neurons results in later-onset progressive degeneration of the cerebellum and severe ataxia

We therefore next examined mice from crosses of the *Calb2*-Cre and *Cask*^{floxed} lines. It has been shown previously that the *Cask*^{floxed} mouse is a hypomorph that expresses ~40% CASK, likely due to a phenomenon known as selection cassette interference [18].

Cask^{floxed} mice are smaller than wild type mice and exhibit cerebellar hypoplasia [13 18 44]. *Cask*^{floxed};*Calb2*-Cre F1 mice were genotyped by PCR.

Cask^{floxed};*Calb2*-Cre mice remain indistinguishable from the *Cask*^{floxed} mice well into adulthood (~40 days), indicating that acute deletion of *Cask* does not have significant effects on cerebellar development, motor learning, or locomotor function. Past two months of age, however, *Cask*^{floxed};*Calb2*-Cre mice begin displaying obvious locomotor incoordination and ataxia which are rapidly progressive. By approximately P100, these mice are profoundly ataxic, are unable to keep their balance and repeatedly fall over with an inability to walk forward (supplemental video). Despite profound motor coordination deficits, the *Cask*^{floxed};*Calb2*-Cre mice are otherwise healthy and display a slick coat, good body condition score, and are bright, alert and responsive. Compared to littermate *Cask*^{floxed} controls, the cerebellum of the *Cask*^{floxed};*Calb2*-Cre mouse is extremely diminished in volume at P100 when the motor phenotype has reached maximum (Figure 4A,B). Comparing the histology of the *Cask*^{floxed};*Calb2*-Cre cerebellum at P30 (well before onset of ataxia) and P100 (after onset of ataxia), our results indicate that at P30, the cerebellum of *Cask*^{floxed};*Calb2*-Cre mice is populated with well-placed granule and Purkinje cells. At P100, however, we observe profound loss of granule cells, whereas Purkinje cells remain visible as a standard single layer of cells (Figure 4C). The molecular layer of the cerebellum is thin and collapsed, most likely due to loss of parallel fibers arising from the granular cells and loss of synaptic connections between granule cells and Purkinje cells (Figure 4D–G). We therefore next quantified synaptic connections within the cerebellar layers using bassoon as a pre-synaptic marker. As seen in Supplemental Figure 12, our data indicate that synapse density is unaltered, although the absolute number of synapses is reduced due to the shrunken volume of the molecular layer. The large number of remaining synapses are likely derived from the climbing fibers. Notably, in our previous studies, we did not observe degeneration of retinal ganglion cells, which are also positive for *Calb2*-Cre [53]. Our data here thus indicate that loss of CASK results in the disproportionate degeneration of a specific vulnerable neuronal population, cerebellar granule cells, leading to cerebellar hypoplasia.

A decrease in grey matter creates an impression of increased white matter area. We therefore quantified myelin in the *Cask*^{floxed};*Calb2*-Cre mice using FluoroMyelin™ staining. As seen in Figure 4H–I, the myelin appears to be disorganized in the white matter of folia from the *Cask*^{floxed};*Calb2*-Cre mouse cerebellum, which is most obvious in the region immediately distal to Purkinje cells. We also observed extremely limited myelinated axons in the anterior-most folium (Figure 4H). Quantification of pixels displayed a strong trend towards a decrease in fluoromyelin staining which did not reach statistical significance (Figure 4I). The degeneration of cerebellar grey matter thus is also associated with disorganization of the white matter in the *Cask*^{floxed};*Calb2*-Cre mouse cerebellum, and the broadened white matter layer is likely to be filled only with acellular matrix. Because the *Cask*^{floxed};*Calb2*-Cre mouse represents a targeted deletion of CASK in cerebellar neuronal cells, it is reasonable to conclude that the observed disordered white matter is a property of the underlying neuronal pathology rather than an oligodendrocyte-mediated pathology, confirming our observations from the human subject.

Neuronal loss or damage is typically associated with gliosis, as seen in the human subject, so we next immunostained mouse cerebella with a marker for reactive gliosis, glial acidic fibrillary protein (GFAP) (Figure 5A). Although *Cask*^{floxed} mice display some GFAP positivity, *Cask*^{floxed};*Calb2*-Cre mice displayed an almost 2-fold higher level of astrogliosis compared to age-matched control *Cask*^{floxed} mice (Figure 5B). Most of the GFAP in these cerebella was associated with Bergmann glia, since the IGL was extremely hypocellular. On staining the Bergmann glia with S100β, we did not see increased immunoreactivity in Bergmann glia or proliferation of Bergmann glia (Figure 5C,F), but we did observe a strong trend of increased S100β reactivity in the IGL extracellular space (Figure 5D, E). S100β is known to be secreted during metabolic stress and functions via binding to a receptor of advanced glycation end products [56 57]. Overall, this finding suggests that CASK loss-of-function produces protracted neuronal loss in the cerebellum, explaining why MICPCH in humans typically becomes obvious a few months after birth. The cerebellar hypoplasia associated with loss of CASK represents disproportionate neuronal loss in the cerebellum.

Finally, we examined the functional loss associated with the cerebellar degeneration in *Cask*^{floxed};Calb2-Cre mice. By P100, the mouse's hindlimbs can no longer maintain normal righting, and the mice display hindlimb clasping with no obvious dystonic movement (Figure 5G). Accelerating rotarod balance experiments suggest that even at P48, the mutant mice have a trend to underperform on a rotarod, indicating that the process of cerebellar degeneration and consequent functional degradation may be ongoing even before obvious locomotor defects are visually noticed within the cage. At P70 the mice are unable to perform on the rotarod at all, demonstrating a rapid degradation of locomotor coordination within a short span of 3 weeks (Figure 5H). Additionally, the cerebellar degeneration and accompanying motor phenotype only manifest in the homozygous knockout of CASK from cerebellar cells and not in the heterozygous deletion (Figure 5G,H and Supplemental Figure 13), despite CASK being absent from approximately half the cells in the heterozygous deletion due to its X-linked nature. This indicates that cerebellar degeneration requires total deletion of CASK in the cerebellum to produce degeneration in a non-cell autonomous fashion [44 53]. Our data additionally suggest that CASK haploinsufficiency is not sufficient to affect the cerebellum after postnatal development. Overall, our data indicate that deletion of CASK does not affect brain development, and the brain phenotype is unlikely due to defects of reelin function. Further, CASK loss leads to degeneration of cerebellar neurons, causing pronounced cerebellar atrophy that results in a progressive cerebellar ataxia.

Discussion

Developmental disorders are defined based on their clinical course rather than cellular pathology. Presentation of a severe, chronic disability (mental and/or physical impairment) in three or more areas of major life activity by the age of 22 that is likely to continue through the individual's lifetime is classified as a developmental disorder (*Developmental Disabilities Assistance and Bill of Rights Act of 2000*). Strategies for molecular therapeutic intervention, however, are more likely to be dependent on cellular pathology rather than the clinical course of a given disorder. Conditions associated with mutations in the human *CASK* gene have been described as developmental disorders [10 12]. *CASK* is a

ubiquitously expressed gene and has been proposed to have a function in a variety of organs including the intestine, kidney, heart and brain [21 22], and mutations in *CASK* produce microcephaly as well as somatic growth retardation [10 12]. In boys who do not express *CASK,* a clear picture has emerged consisting of neurological devastation, microcephaly, pontocerebellar hypoplasia (PCH), and a consistently abnormal EEG pattern characterized by disorganization, low frequency, attenuation and discontinuity. *CASK* null boys are thus likely to be diagnosed with epileptic encephalopathies such as Ohtahara syndrome and West syndrome. Despite uniform neurological findings in these subjects, findings involving other organ systems remain inconsistent and often unremarkable. Our analysis of *CASK* null mutations in boys indicates that the function/s of CASK that are critical for survival are brain-specific; all other organ systems can function within the normal range without CASK [16]. In fact, we have previously demonstrated that deletion of *CASK* in neurons is sufficient to produce somatic and brain size reduction in mice [44]. The thinning and dysfunction of the brain stem manifests as aberrant respiratory, deglutition and cardiovascular reflexes, and it is this dysfunction that underlies the lethality associated with CASK loss in mammals [16 18].

Neurodevelopment could be stalled at several steps of brain development. This includes cell proliferation, neuronal differentiation and polarization, neuronal migration and final neuronal maturation including axonal and dendritic growth and synaptogenesis. At a molecular level CASK has been proposed to play a role in all these processes. Evidence exists to suggest that CASK participates in mitotic spindle orientation and cell proliferation [58], in cell polarization [23], and in axonal and dendritic maturation and synaptogenesis [28 29 31]. Within the synapse, CASK can be found in molecular complexes that include other important molecules like Mint1, Caskin, liprin-α and the adhesion molecule neurexin [21 59–61]. CASK is a kinase that phosphorylates neurexin and is likely to regulate this complex formation [60 62–64]. The most accepted notion of CASK in neurodevelopment has, however, been the role of CASK in neuronal migration via its interaction with CINAP and Tbr-1, resulting in the upregulation of reelin transcription [13 33 34 65]. Surprisingly, our analysis of the CASK-null human brain does not support any of these putative roles of CASK in neurodevelopment.

Genetic manipulation of *Cask* in murine models has demonstrated that CASK-linked murine brain pathology is postnatal and not likely to be a developmental defect [44 53]. Although the delivery of the decedent described here was late preterm, Apgar scores were normal, and the infant was released from the hospital without concern. Rapid regression within days to weeks has been noted in this and other boys with *CASK*-null mutations, indicating that although degeneration may begin in the third trimester, it continues rapidly throughout infancy. Despite a smaller size, the gross and histological findings in a brain without CASK are minimal. Overall, the brain configuration, vasculature, ventricular system, meninges, brain lamination, and neuronal migration all remained unaltered. The decrease in foliation noted in the decedent's cerebellum is likely explained by the rapid loss of granule cells after migration that precludes the formation of a densely packed IGL, a critical step for inducing foliation [66 67], although we cannot strictly exclude specific developmental disruptions in the formation of 'anchoring centers' required for foliation [67]. Overall our data indicate that in the presence of *CASK* mutation, embryonic brain development appears unchanged, with

no defect in neuronal differentiation and migration. The findings from neuroimaging and histological studies of human cases are consistent with findings from CASK knockout mice where brain size, lamination, and synapse formation are all normal at birth [18]. In fact, the absence of an acute locomotor effect in *Cask*^{floxed};*Calb2*-Cre mice excludes a synaptic role of CASK in cerebellar function. Importantly, our study here strongly suggests that CASK does not play a role in neurodevelopment via the purported Tbr-1-reelin pathway. This interpretation is in line with the observation that in the mouse model, abrogation of the CASK-Tbr-1 interaction does not affect brain size or lamination [41]. A number of CASK missense mutations have been identified that are associated with intellectual disability and MICPCH. Recent studies on these missense mutations have also indicated that the CASK-Tbr-1 interaction does not play a role in MICPCH [11 68].

In girls with heterozygous *CASK* mutations, the predominant manifestations are also brain-related [10 12]. Our data presented here demonstrate that although *Cask*$^{+/-}$ mice have cerebellar hypoplasia, they do not significantly degenerate further in old age, which agrees with the clinical definition of a neurodevelopmental disease. In girls with MICPCH and in *Cask*$^{+/-}$ mice, however, ~50% of cells still express CASK [44 65], confounding the study of neuropathology and making it difficult to draw firm conclusions. Conditional genetic animal model experimentation allows us to overcome the difficulties presented by this X-linked condition and also helps separate the neurodegenerative pathology of CASK loss from developmental contributions.

CASK deletion in mice is lethal, making postnatal developmental studies in a whole-body knockout model impossible. We have, however, previously demonstrated that CASK does not play a role in maturation and migration of cerebellar neurons by deleting CASK specifically in a distributed subpopulation of granule cells and maturing Purkinje cells [44]. In the current work, we have generated otherwise healthy mice that do not express *Cask* in many parts of the brain, including the post-migratory cerebellar neurons, allowing us to clearly demonstrate that lack of CASK produces cerebellar atrophy through granule cell degeneration. This granule cell degeneration likely underlies MICPCH. CASK has previously been identified as a biomarker for several neurodegenerative disorders [69–72]; our study thus explains these previous unbiased findings. CASK loss, however, does not uniformly produce neurodegeneration; for example, loss of CASK is also associated with optic nerve hypoplasia, but unexpectedly, CASK deletion from retinal ganglion cells (whose axons form the optic nerve) does not negatively affect optic nerve pathology in mice of the same genotype [53]. Similarly, *Calb2* is present in many cortical interneurons and neurons of the olfactory bulb, hippocampus and striatum, but we do not observe severe atrophy of these regions in the *Cask*^{floxed};*Calb2*-Cre mice (Figure 4A). In fact, a closer look within the cerebellum suggests that cerebellar degeneration may be primarily due to granule cell death, making this condition most similar to Norman-type cerebellar atrophy (OMIM: 213200). Many Purkinje cells, which are among the first cerebellar cells to express *Calb2*-Cre, do not die off but rather persist throughout the lifespan, even following the appearance of ataxia. Thus CASK loss apparently affects neurons differentially.

PCH pathologies are typically thought to be neurodegenerative beginning antenatally [46]. Defects in both energy production and protein metabolism (specifically, protein synthesis)

are known to disproportionately affect the cerebellum and are likely causes of PCH [73]. In the case of CASK mutation, PCH has been described as neurodevelopmental, mostly due to the non-progressive course seen in females [74]. In contrast to hemizygous and homozygous *Cask*^{floxed};*Calb2*-Cre mice, the heterozygous *Cask*^{floxed};*Calb2*-Cre mice fail to exhibit cerebellar degeneration (Supplemental Figure 13). Our findings here thus suggest that CASK-linked PCH is also neurodegenerative, and the arrest of neurodegeneration in girls most likely arises from mosaicism of the defective X-linked gene, which guarantees that ~50% of brain cells retain a normally functioning *CASK* gene (Figure 6). Mechanistically, our findings demonstrate that CASK is also likely to function in pathways associated with energy production and protein metabolism [44 75], confirming that MICPCH shares not only the pathogenic mechanism, but also a common molecular pathway, with other types of PCH.

Heterozygous mutations in X-linked genes other than *CASK*, such as MeCP2 and CDKL5, are associated with postnatal microcephaly in girls [1]. Intriguingly, subjects with mutations in these genes show an initial normal developmental trajectory followed by developmental arrest and delay (regression) [76 77]. Mutational analysis of orthologous genes in murine models also reveal phenotypes which are clearly post-developmental, presenting only in adulthood [78] [79]. Incidentally, just like CASK mutations, CDKL5 and MeCP2 mutations in males are associated with epileptic encephalopathy [2 3]. These data raise the possibility that even in disorders such as Rett syndrome (MeCP2 mutation) and CDKL5 deficiency, the pathology may be neurodegenerative, as originally suggested by Andreas Rett [5], but the clinical course may not be progressive in females due to the mosaic expression of the normal gene under heterozygous conditions.

Supplementary Material

Refer to Web version on PubMed Central for supplementary material.

Acknowledgements:

We thank Drs. Thomas Südhof and Alexei Morozov for providing CASK^{floxed} mice and Ai14-LSL-tdTomato mice, respectively.

Funding:

The work was supported with funding from the NIH National Eye Institute (R01EY024712) and Angelina CASK Neurological Research Foundation to KM, and from the NIH National Institute of Neurological Disorders and Stroke grant (R01NS117698) to S.S.

References

1. Seltzer LE, Paciorkowski AR. Genetic disorders associated with postnatal microcephaly. Am J Med Genet C Semin Med Genet 2014;166C(2):140–55 doi: 10.1002/ajmg.c.31400[published Online First: Epub Date]|. [PubMed: 24839169]
2. Jakimiec M, Paprocka J, Smigiel R. CDKL5 Deficiency Disorder-A Complex Epileptic Encephalopathy. Brain Sci 2020;10(2) doi: 10.3390/brainsci10020107[published Online First: Epub Date]|.
3. Kankirawatana P, Leonard H, Ellaway C, Scurlock J, Mansour A, Makris CM, Dure LSt,Friez M, Lane J, Kiraly-Borri C, Fabian V, Davis M, Jackson J, Christodoulou J, Kaufmann WE,

Ravine D, Percy AK. Early progressive encephalopathy in boys and MECP2 mutations. Neurology 2006;67(1):164–6 doi: 10.1212/01.wnl.0000223318.28938.45[published Online First: Epub Date]|. [PubMed: 16832102]

4. Saitsu H, Kato M, Osaka H, Moriyama N, Horita H, Nishiyama K, Yoneda Y, Kondo Y, Tsurusaki Y, Doi H, Miyake N, Hayasaka K, Matsumoto N. CASK aberrations in male patients with Ohtahara syndrome and cerebellar hypoplasia. Epilepsia 2012;53(8):1441–49 doi: 10.1111/j.1528-1167.2012.03548.x[published Online First: Epub Date]|. [PubMed: 22709267]
5. Rett A. [On a unusual brain atrophy syndrome in hyperammonemia in childhood]. Wien Med Wochenschr 1966;116(37):723–6 [PubMed: 5300597]
6. FitzGerald PM, Jankovic J, Glaze DG, Schultz R, Percy AK. Extrapyramidal involvement in Rett's syndrome. Neurology 1990;40(2):293–5 doi: 10.1212/wnl.40.2.293[published Online First: Epub Date]|. [PubMed: 2073236]
7. Neul JL, Zoghbi HY. Rett syndrome: a prototypical neurodevelopmental disorder. Neuroscientist 2004;10(2):118–28 doi: 10.1177/1073858403260995[published Online First: Epub Date]|. [PubMed: 15070486]
8. Zoghbi HY. Postnatal neurodevelopmental disorders: meeting at the synapse? Science 2003;302(5646):826–30 doi: 10.1126/science.1089071[published Online First: Epub Date]|. [PubMed: 14593168]
9. Schule B, Armstrong DD, Vogel H, Oviedo A, Francke U. Severe congenital encephalopathy caused by MECP2 null mutations in males: central hypoxia and reduced neuronal dendritic structure. Clin Genet 2008;74(2):116–26 doi: 10.1111/j.1399-0004.2008.01005.x[published Online First: Epub Date]|. [PubMed: 18477000]
10. Burglen L, Chantot-Bastaraud S, Garel C, Milh M, Touraine R, Zanni G, Petit F, Afenjar A, Goizet C, Barresi S, Coussement A, Ioos C, Lazaro L, Joriot S, Desguerre I, Lacombe D, des Portes V, Bertini E, Siffroi JP, de Villemeur TB, Rodriguez D. Spectrum of pontocerebellar hypoplasia in 13 girls and boys with CASK mutations: confirmation of a recognizable phenotype and first description of a male mosaic patient. Orphanet J Rare Dis 2012;7:18 doi: 1750–1172-7–18 [pii] 10.1186/1750-1172-7-18[published Online First: Epub Date]|. [PubMed: 22452838]
11. LaConte LEW, Chavan V, Elias AF, Hudson C, Schwanke C, Styren K, Shoof J, Kok F, Srivastava S, Mukherjee K. Two microcephaly-associated novel missense mutations in CASK specifically disrupt the CASK-neurexin interaction. Hum Genet 2018;137(3):231–46 doi: 10.1007/s00439-018-1874-3[published Online First: Epub Date]|. [PubMed: 29426960]
12. Moog U, Kutsche K, Kortum F, Chilian B, Bierhals T, Apeshiotis N, Balg S, Chassaing N, Coubes C, Das S, Engels H, Van Esch H, Grasshoff U, Heise M, Isidor B, Jarvis J, Koehler U, Martin T, Oehl-Jaschkowitz B, Ortibus E, Pilz DT, Prabhakar P, Rappold G, Rau I, Rettenberger G, Schluter G, Scott RH, Shoukier M, Wohlleber E, Zirn B, Dobyns WB, Uyanik G. Phenotypic spectrum associated with CASK loss-of-function mutations. J Med Genet 2011;48(11):741–51 doi: jmedgenet-2011–100218 [pii] 10.1136/jmedgenet-2011-100218[published Online First: Epub Date]|. [PubMed: 21954287]
13. Najm J, Horn D, Wimplinger I, Golden JA, Chizhikov VV, Sudi J, Christian SL, Ullmann R, Kuechler A, Haas CA, Flubacher A, Charnas LR, Uyanik G, Frank U, Klopocki E, Dobyns WB, Kutsche K. Mutations of CASK cause an X-linked brain malformation phenotype with microcephaly and hypoplasia of the brainstem and cerebellum. Nat Genet 2008;40(9):1065–7 doi: 10.1038/ng.194[published Online First: Epub Date]|. [PubMed: 19165920]
14. Takanashi J, Okamoto N, Yamamoto Y, Hayashi S, Arai H, Takahashi Y, Maruyama K, Mizuno S, Shimakawa S, Ono H, Oyanagi R, Kubo S, Barkovich AJ, Inazawa J. Clinical and radiological features of Japanese patients with a severe phenotype due to CASK mutations. Am J Med Genet A 2012;158A(12):3112–8 doi: 10.1002/ajmg.a.35640[published Online First: Epub Date]|. [PubMed: 23165780]
15. Moog U, Bierhals T, Brand K, Bautsch J, Biskup S, Brune T, Denecke J, de Die-Smulders CE, Evers C, Hempel M, Henneke M, Yntema H, Menten B, Pietz J, Pfundt R, Schmidtke J, Steinemann D, Stumpel CT, Van Maldergem L, Kutsche K. Phenotypic and molecular insights into CASK-related disorders in males. Orphanet J Rare Dis 2015;10:44 doi: 10.1186/s13023-015-0256-3[published Online First: Epub Date]|. [PubMed: 25886057]

16. Mukherjee K, Patel PA, Rajan DS, LaConte LEW, Srivastava S. Survival of a male patient harboring CASK Arg27Ter mutation to adolescence. Mol Genet Genomic Med 2020:e1426 doi: 10.1002/mgg3.1426[published Online First: Epub Date]|. [PubMed: 32696595]

17. Nishio Y, Kidokoro H, Takeo T, Narita H, Sawamura F, Narita K, Kawano Y, Nakata T, Muramatsu H, Hara S, Kaname T, Natsume J. The eldest case of MICPCH with CASK mutation exhibiting gross motor regression. Brain Dev 2020 doi: 10.1016/j.braindev.2020.11.007[published Online First: Epub Date]|.

18. Atasoy D, Schoch S, Ho A, Nadasy KA, Liu XR, Zhang WQ, Mukherjee K, Nosyreva ED, Fernandez-Chacon R, Missler M, Kavalali ET, Sudhof TC. Deletion of CASK in mice is lethal and impairs synaptic function. P Natl Acad Sci USA 2007;104(7):2525–30 doi: 10.1073/pnas.0611003104[published Online First: Epub Date]|.

19. Xue L, Cai JY, Ma J, Huang Z, Guo MX, Fu LZ, Shi YB, Li WX. Global expression profiling reveals genetic programs underlying the developmental divergence between mouse and human embryogenesis. BMC Genomics 2013;14:568 doi: 10.1186/1471-2164-14-568[published Online First: Epub Date]|. [PubMed: 23961710]

20. O'Rahilly R, Muller F. Developmental stages in human embryos: revised and new measurements. Cells Tissues Organs 2010;192(2):73–84 doi: 10.1159/000289817[published Online First: Epub Date]|. [PubMed: 20185898]

21. Hata Y, Butz S, Sudhof TC. CASK: a novel dlg/PSD95 homolog with an N-terminal calmodulin-dependent protein kinase domain identified by interaction with neurexins. J Neurosci 1996;16(8):2488–94 [PubMed: 8786425]

22. Stevenson D, Laverty HG, Wenwieser S, Douglas M, Wilson JB. Mapping and expression analysis of the human CASK gene. Mamm Genome 2000;11(10):934–7 doi: 10.1007/s003350010170 [pii] [published Online First: Epub Date]|. [PubMed: 11003712]

23. Caruana G. Genetic studies define MAGUK proteins as regulators of epithelial cell polarity. Int J Dev Biol 2002;46(4):511–8 [PubMed: 12141438]

24. Beaudreuil S, Zhang X, Herr F, Harper F, Candelier JJ, Fan Y, Yeter H, Dudreuilh C, Lecru L, Vazquez A, Charpentier B, Lorenzo HK, Durrbach A. Circulating CASK is associated with recurrent focal segmental glomerulosclerosis after transplantation. PLoS One 2019;14(7):e0219353 doi: 10.1371/journal.pone.0219353[published Online First: Epub Date]|. [PubMed: 31356645]

25. Ahn SY, Kim Y, Kim ST, Swat W, Miner JH. Scaffolding proteins DLG1 and CASK cooperate to maintain the nephron progenitor population during kidney development. J Am Soc Nephrol 2013;24(7):1127–38 doi: 10.1681/ASN.2012111074[published Online First: Epub Date]|. [PubMed: 23661808]

26. Eichel CA, Beuriot A, Chevalier MY, Rougier JS, Louault F, Dilanian G, Amour J, Coulombe A, Abriel H, Hatem SN, Balse E. Lateral Membrane-Specific MAGUK CASK Down-Regulates NaV1.5 Channel in Cardiac Myocytes. Circ Res 2016;119(4):544–56 doi: 10.1161/CIRCRESAHA.116.309254[published Online First: Epub Date]|. [PubMed: 27364017]

27. Beuriot A, Eichel CA, Dilanian G, Louault F, Melgari D, Doisne N, Coulombe A, Hatem SN, Balse E. Distinct calcium/calmodulin-dependent serine protein kinase domains control cardiac sodium channel membrane expression and focal adhesion anchoring. Heart Rhythm 2020;17(5 Pt A):786–94 doi: 10.1016/j.hrthm.2019.12.019[published Online First: Epub Date]|. [PubMed: 31904424]

28. Kuo TY, Hong CJ, Chien HL, Hsueh YP. X-linked mental retardation gene CASK interacts with Bcl11A/CTIP1 and regulates axon branching and outgrowth. J Neurosci Res 2010;88(11):2364–73 doi: 10.1002/jnr.22407[published Online First: Epub Date]|. [PubMed: 20623620]

29. Gao R, Piguel NH, Melendez-Zaidi AE, Martin-de-Saavedra MD, Yoon S, Forrest MP, Myczek K, Zhang G, Russell TA, Csernansky JG, Surmeier DJ, Penzes P. CNTNAP2 stabilizes interneuron dendritic arbors through CASK. Mol Psychiatry 2018;23(9):1832–50 doi: 10.1038/s41380-018-0027-3[published Online First: Epub Date]|. [PubMed: 29610457]

30. Chao HW, Hong CJ, Huang TN, Lin YL, Hsueh YP. SUMOylation of the MAGUK protein CASK regulates dendritic spinogenesis. J Cell Biol 2008;182(1):141–55 doi: 10.1083/jcb.200712094[published Online First: Epub Date]|. [PubMed: 18606847]

31. Samuels BA, Hsueh YP, Shu T, Liang H, Tseng HC, Hong CJ, Su SC, Volker J, Neve RL, Yue DT, Tsai LH. Cdk5 promotes synaptogenesis by regulating the subcellular distribution of the MAGUK family member CASK. Neuron 2007;56(5):823–37 doi: S0896–6273(07)00769–6 [pii] 10.1016/j.neuron.2007.09.035[published Online First: Epub Date]|. [PubMed: 18054859]
32. Wang TF, Ding CN, Wang GS, Luo SC, Lin YL, Ruan Y, Hevner R, Rubenstein JL, Hsueh YP. Identification of Tbr-1/CASK complex target genes in neurons. J Neurochem 2004;91(6):1483–92 doi: 10.1111/j.1471-4159.2004.02845.x[published Online First: Epub Date]|. [PubMed: 15584924]
33. Wang GS, Hong CJ, Yen TY, Huang HY, Ou Y, Huang TN, Jung WG, Kuo TY, Sheng M, Wang TF, Hsueh YP. Transcriptional modification by a CASK-interacting nucleosome assembly protein. Neuron 2004;42(1):113–28 doi: 10.1016/s0896-6273(04)00139-4[published Online First: Epub Date]|. [PubMed: 15066269]
34. Hsueh YP, Wang TF, Yang FC, Sheng M. Nuclear translocation and transcription regulation by the membrane-associated guanylate kinase CASK/LIN-2. Nature 2000;404(6775):298–302 doi: 10.1038/35005118[published Online First: Epub Date]|. [PubMed: 10749215]
35. Bredt DS. Cell biology. Reeling CASK into the nucleus. Nature 2000;404(6775):241–2 doi: 10.1038/35005208[published Online First: Epub Date]|. [PubMed: 10749196]
36. Hirotsune S, Takahara T, Sasaki N, Hirose K, Yoshiki A, Ohashi T, Kusakabe M, Murakami Y, Muramatsu M, Watanabe S, Nakao K, Katsuki M, Hayashizaki Y. The reeler gene encodes a protein with an EGF-like motif expressed by pioneer neurons. Nat Genet 1995;10(1):77–83 doi: 10.1038/ng0595-77[published Online First: Epub Date]|. [PubMed: 7647795]
37. Hamburgh M. Analysis of the Postnatal Developmental Effects of “Reeler,” a Neurological Mutation in Mice. A Study in Developmental Genetics. Dev Biol 1963;8:165–85 doi: 10.1016/0012-1606(63)90040-x[published Online First: Epub Date]|. [PubMed: 14069672]
38. Hevner RF, Shi L, Justice N, Hsueh Y, Sheng M, Smiga S, Bulfone A, Goffinet AM, Campagnoni AT, Rubenstein JL. Tbr1 regulates differentiation of the preplate and layer 6. Neuron 2001;29(2):353–66 doi: 10.1016/s0896-6273(01)00211-2[published Online First: Epub Date]|. [PubMed: 11239428]
39. Namavar Y, Barth PG, Baas F, Poll-The BT. Reply: Mutations of TSEN and CASK genes are prevalent in pontocerebellar hypoplasias type 2 and 4. Brain 2012;135(1):e200–e00
40. Takanashi J, Arai H, Nabatame S, Hirai S, Hayashi S, Inazawa J, Okamoto N, Barkovich AJ. Neuroradiologic features of CASK mutations. AJNR Am J Neuroradiol 2010;31(9):1619–22 doi: ajnr.A2173 [pii] 10.3174/ajnr.A2173[published Online First: Epub Date]|. [PubMed: 20595373]
41. Huang TN, Hsueh YP. Calcium/calmodulin-dependent serine protein kinase (CASK), a protein implicated in mental retardation and autism-spectrum disorders, interacts with T-Brain-1 (TBR1) to control extinction of associative memory in male mice. J Psychiatry Neurosci 2017;42(1):37–47 doi: 10.1503/jpn.150359[published Online First: Epub Date]|. [PubMed: 28234597]
42. Sando R, Bushong E, Zhu Y, Huang M, Considine C, Phan S, Ju S, Uytiepo M, Ellisman M, Maximov A. Assembly of Excitatory Synapses in the Absence of Glutamatergic Neurotransmission. Neuron 2017;94(2):312–21 e3 doi: 10.1016/j.neuron.2017.03.047[published Online First: Epub Date]|. [PubMed: 28426966]
43. Verhage M, Maia AS, Plomp JJ, Brussaard AB, Heeroma JH, Vermeer H, Toonen RF, Hammer RE, van den Berg TK, Missler M, Geuze HJ, Sudhof TC. Synaptic assembly of the brain in the absence of neurotransmitter secretion. Science 2000;287(5454):864–9 doi: 10.1126/science.287.5454.864[published Online First: Epub Date]|. [PubMed: 10657302]
44. Srivastava S, McMillan R, Willis J, Clark H, Chavan V, Liang C, Zhang H, Hulver M, Mukherjee K. X-linked intellectual disability gene CASK regulates postnatal brain growth in a non-cell autonomous manner. Acta Neuropathol Commun 2016;4:30 doi: 10.1186/s40478-016-0295-6[published Online First: Epub Date]|. [PubMed: 27036546]
45. Cendelin J. From mice to men: lessons from mutant ataxic mice. Cerebellum & ataxias 2014;1(1):1–21 [PubMed: 26331025]
46. van Dijk T, Barth P, Baas F, Reneman L, Poll-The BT. Postnatal Brain Growth Patterns in Pontocerebellar Hypoplasia. Neuropediatrics 2020 doi: 10.1055/s-0040-1716900[published Online First: Epub Date]|.

47. Wang Y, Wang C, Ranefall P, Broussard GJ, Wang Y, Shi G, Lyu B, Wu CT, Wang Y, Tian L, Yu G. SynQuant: an automatic tool to quantify synapses from microscopy images. Bioinformatics 2020;36(5):1599–606 doi: 10.1093/bioinformatics/btz760[published Online First: Epub Date]|. [PubMed: 31596456]
48. Tissir F, Goffinet AM. Reelin and brain development. Nature Reviews Neuroscience 2003;4(6):496–505 [PubMed: 12778121]
49. Sarnat HB, Flores-Sarnat L, Auer RN. Synaptogenesis in the foetal and neonatal cerebellar system. 2. Pontine nuclei and cerebellar cortex. Dev Neurosci 2013;35(4):317–25 doi: 10.1159/000351031[published Online First: Epub Date]|. [PubMed: 23796553]
50. Ichikawa R, Yamasaki M, Miyazaki T, Konno K, Hashimoto K, Tatsumi H, Inoue Y, Kano M, Watanabe M. Developmental switching of perisomatic innervation from climbing fibers to basket cell fibers in cerebellar Purkinje cells. J Neurosci 2011;31(47):16916–27 doi: 10.1523/JNEUROSCI.2396-11.2011[published Online First: Epub Date]|. [PubMed: 22114262]
51. Perry VH, Nicoll JA, Holmes C. Microglia in neurodegenerative disease. Nat Rev Neurol 2010;6(4):193–201 doi: 10.1038/nrneurol.2010.17[published Online First: Epub Date]|. [PubMed: 20234358]
52. Sarnat HB, Flores-Sarnat L, Auer RN. Sequence of synaptogenesis in the fetal and neonatal cerebellar system - part 1: Guillain-Mollaret triangle (dentato-rubro-olivo-cerebellar circuit). Dev Neurosci 2013;35(1):69–81 doi: 10.1159/000350503[published Online First: Epub Date]|. [PubMed: 23689557]
53. Kerr A, Patel PA, LaConte LEW, Liang C, Chen CK, Shah V, Fox MA, Mukherjee K. Non-Cell Autonomous Roles for CASK in Optic Nerve Hypoplasia. Invest Ophthalmol Vis Sci 2019;60(10):3584–94 doi: 10.1167/iovs.19-27197[published Online First: Epub Date]|. [PubMed: 31425583]
54. Schiffmann SN, Cheron G, Lohof A, d'Alcantara P, Meyer M, Parmentier M, Schurmans S. Impaired motor coordination and Purkinje cell excitability in mice lacking calretinin. Proc Natl Acad Sci U S A 1999;96(9):5257–62 doi: 10.1073/pnas.96.9.5257[published Online First: Epub Date]|. [PubMed: 10220453]
55. Bearzatto B, Servais L, Roussel C, Gall D, Baba-Aissa F, Schurmans S, de Kerchove d'Exaerde A, Cheron G, Schiffmann SN. Targeted calretinin expression in granule cells of calretinin-null mice restores normal cerebellar functions. FASEB J 2006;20(2):380–2 doi: 10.1096/fj.05-3785fje[published Online First: Epub Date]|. [PubMed: 16352645]
56. Zglejc-Waszak K, Mukherjee K, Juranek JK. The cross-talk between RAGE and DIAPH1 in neurological complications of diabetes: A review. Eur J Neurosci 2021;54(6):5982–99 doi: 10.1111/ejn.15433[published Online First: Epub Date]|. [PubMed: 34449932]
57. Gerlach R, Demel G, Konig HG, Gross U, Prehn JH, Raabe A, Seifert V, Kogel D. Active secretion of S100B from astrocytes during metabolic stress. Neuroscience 2006;141(4):1697–701 doi: 10.1016/j.neuroscience.2006.05.008[published Online First: Epub Date]|. [PubMed: 16782283]
58. Porter AP, White GRM, Mack NA, Malliri A. The interaction between CASK and the tumour suppressor Dlg1 regulates mitotic spindle orientation in mammalian epithelia. J Cell Sci 2019;132(14) doi: 10.1242/jcs.230086[published Online First: Epub Date]|.
59. Butz S, Okamoto M, Sudhof TC. A tripartite protein complex with the potential to couple synaptic vesicle exocytosis to cell adhesion in brain. Cell 1998;94(6):773–82 [PubMed: 9753324]
60. LaConte LE, Chavan V, Liang C, Willis J, Schonhense EM, Schoch S, Mukherjee K. CASK stabilizes neurexin and links it to liprin-alpha in a neuronal activity-dependent manner. Cell Mol Life Sci 2016;73(18):3599–621 doi: 10.1007/s00018-016-2183-4[published Online First: Epub Date]|. [PubMed: 27015872]
61. Tabuchi K, Biederer T, Butz S, Sudhof TC. CASK participates in alternative tripartite complexes in which Mint 1 competes for binding with caskin 1, a novel CASK-binding protein. J Neurosci 2002;22(11):4264–73 doi: 20026421[published Online First: Epub Date]|. [PubMed: 12040031]
62. Cortese GP, Zhu M, Williams D, Heath S, Waites CL. Parkin Deficiency Reduces Hippocampal Glutamatergic Neurotransmission by Impairing AMPA Receptor Endocytosis. J Neurosci 2016;36(48):12243–58 doi: 10.1523/JNEUROSCI.1473-16.2016[published Online First: Epub Date]|. [PubMed: 27903732]

63. Mukherjee K, Sharma M, Jahn R, Wahl MC, Sudhof TC. Evolution of CASK into a Mg2+-Sensitive Kinase. Sci Signal 2010;3(119) doi: ARTN ra33 10.1126/scisignal.2000800[published Online First: Epub Date]|.
64. Mukherjee K, Sharma M, Urlaub H, Bourenkov GP, Jahn R, Sudhof TC, Wahl MC. CASK functions as a Mg2+-independent neurexin kinase. Cell 2008;133(2):328–39 doi: 10.1016/j.cell.2008.02.036[published Online First: Epub Date]|. [PubMed: 18423203]
65. Mori T, Kasem EA, Suzuki-Kouyama E, Cao X, Li X, Kurihara T, Uemura T, Yanagawa T, Tabuchi K. Deficiency of calcium/calmodulin-dependent serine protein kinase disrupts the excitatory-inhibitory balance of synapses by down-regulating GluN2B. Mol Psychiatry 2019;24(7):1079–92 doi: 10.1038/s41380-018-0338-4[published Online First: Epub Date]|. [PubMed: 30610199]
66. TAKEDA H, KAMEO Y, YAMAGUCHI T, NAKAJIMA K, ADACHI T. Cerebellar foliation via non-uniform cell accumulation caused by fiber-guided migration of granular cells. Journal of Biomechanical Science and Engineering 2021;16(1):20–00516–20–16
67. Sudarov A, Joyner AL. Cerebellum morphogenesis: the foliation pattern is orchestrated by multi-cellular anchoring centers. Neural development 2007;2(1):1–22 [PubMed: 17207270]
68. Pan YE, Tibbe D, Harms FL, Reissner C, Becker K, Dingmann B, Mirzaa G, Kattentidt-Mouravieva AA, Shoukier M, Aggarwal S, Missler M, Kutsche K, Kreienkamp HJ. Missense mutations in CASK, coding for the calcium-/calmodulin-dependent serine protein kinase, interfere with neurexin binding and neurexin-induced oligomerization. J Neurochem 2021;157(4):1331–50 doi: 10.1111/jnc.15215[published Online First: Epub Date]|. [PubMed: 33090494]
69. Strand AD, Aragaki AK, Shaw D, Bird T, Holton J, Turner C, Tapscott SJ, Tabrizi SJ, Schapira AH, Kooperberg C, Olson JM. Gene expression in Huntington's disease skeletal muscle: a potential biomarker. Hum Mol Genet 2005;14(13):1863–76 doi: 10.1093/hmg/ddi192[published Online First: Epub Date]|. [PubMed: 15888475]
70. Arefin AS, Mathieson L, Johnstone D, Berretta R, Moscato P. Unveiling clusters of RNA transcript pairs associated with markers of Alzheimer's disease progression. PLoS One 2012;7(9):e45535 doi: 10.1371/journal.pone.0045535[published Online First: Epub Date]|. [PubMed: 23029078]
71. Morello G, Guarnaccia M, Spampinato AG, Salomone S, D'Agata V, Conforti FL, Aronica E, Cavallaro S. Integrative multi-omic analysis identifies new drivers and pathways in molecularly distinct subtypes of ALS. Sci Rep 2019;9(1):9968 doi: 10.1038/s41598-019-46355-w[published Online First: Epub Date]|. [PubMed: 31292500]
72. George G, Singh S, Lokappa SB, Varkey J. Gene co-expression network analysis for identifying genetic markers in Parkinson's disease - a three-way comparative approach. Genomics 2018 doi: 10.1016/j.ygeno.2018.05.005[published Online First: Epub Date]|.
73. Kasher PR, Namavar Y, van Tijn P, Fluiter K, Sizarov A, Kamermans M, Grierson AJ, Zivkovic D, Baas F. Impairment of the tRNA-splicing endonuclease subunit 54 (tsen54) gene causes neurological abnormalities and larval death in zebrafish models of pontocerebellar hypoplasia. Hum Mol Genet 2011;20(8):1574–84 doi: 10.1093/hmg/ddr034 ddr034 [pii][published Online First: Epub Date]|. [PubMed: 21273289]
74. van Dijk T, Baas F, Barth PG, Poll-The BT. What's new in pontocerebellar hypoplasia? An update on genes and subtypes. Orphanet J Rare Dis 2018;13(1):92 doi: 10.1186/s13023-018-0826-2[published Online First: Epub Date]|. [PubMed: 29903031]
75. Patel PA, Liang C, Arora A, Vijayan S, Ahuja S, Wagley PK, Settlage R, LaConte LEW, Goodkin HP, Lazar I, Srivastava S, Mukherjee K. Haploinsufficiency of X-linked intellectual disability gene CASK induces post-transcriptional changes in synaptic and cellular metabolic pathways. Exp Neurol 2020;329:113319 doi: 10.1016/j.expneurol.2020.113319[published Online First: Epub Date]|. [PubMed: 32305418]
76. Hagberg B, Aicardi J, Dias K, Ramos O. A progressive syndrome of autism, dementia, ataxia, and loss of purposeful hand use in girls: Rett's syndrome: report of 35 cases. Ann Neurol 1983;14(4):471–9 doi: 10.1002/ana.410140412[published Online First: Epub Date]|. [PubMed: 6638958]
77. Fehr S, Wilson M, Downs J, Williams S, Murgia A, Sartori S, Vecchi M, Ho G, Polli R, Psoni S, Bao X, de Klerk N, Leonard H, Christodoulou J. The CDKL5 disorder is an independent clinical entity associated with early-onset encephalopathy. Eur J Hum Genet 2013;21(3):266–73 doi: 10.1038/ejhg.2012.156[published Online First: Epub Date]|. [PubMed: 22872100]

78. Guy J, Hendrich B, Holmes M, Martin JE, Bird A. A mouse Mecp2-null mutation causes neurological symptoms that mimic Rett syndrome. Nat Genet 2001;27(3):322–6 doi: 10.1038/85899[published Online First: Epub Date]|. [PubMed: 11242117]

79. Montgomery KR, Louis Sam Titus ASC, Wang L, D'Mello SR. Elevated MeCP2 in Mice Causes Neurodegeneration Involving Tau Dysregulation and Excitotoxicity: Implications for the Understanding and Treatment of MeCP2 Triplication Syndrome. Mol Neurobiol 2018;55(12):9057–74 doi: 10.1007/s12035-018-1046-4[published Online First: Epub Date]|. [PubMed: 29637441]

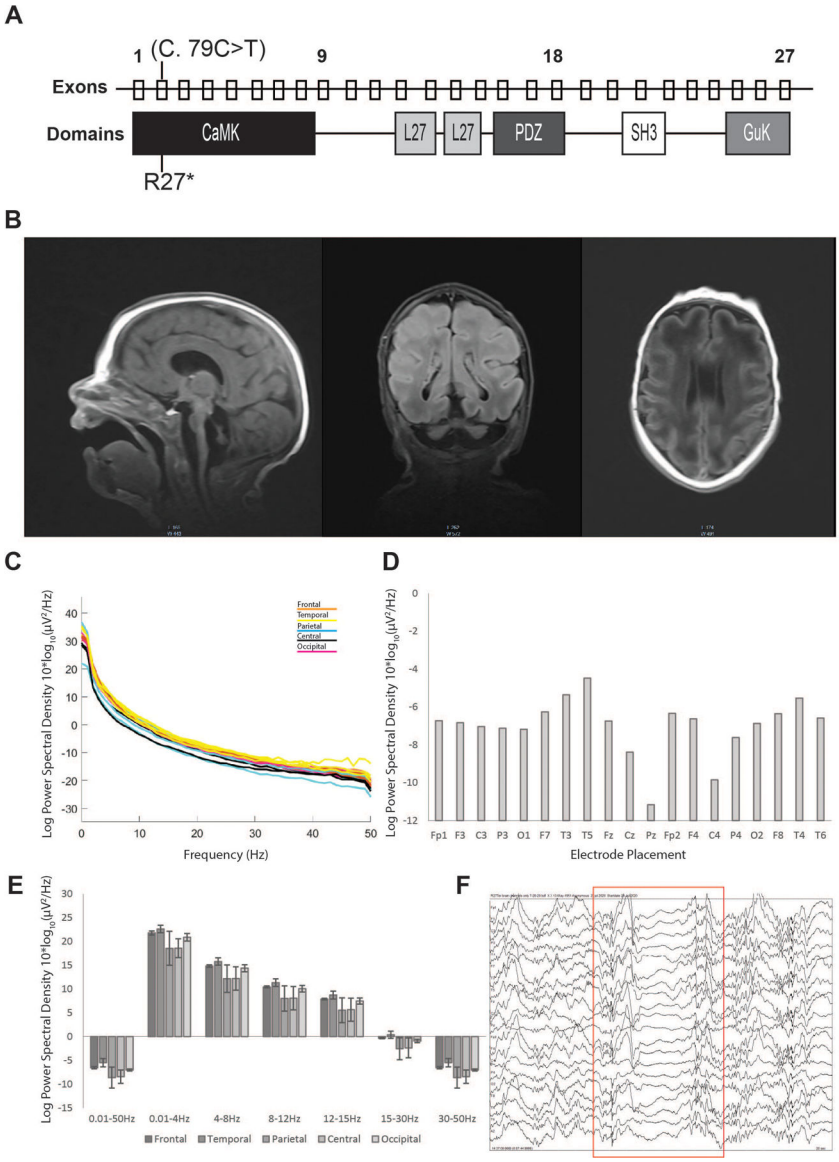

Figure 1. The R27Ter mutation results in early truncation of *CASK*, pontocerebellar hypoplasia, and slowed EEG in a human subject.

A) Location of the R27Ter mutation in the male decedent; top row: exons of the human *CASK* gene; bottom row: corresponding CASK protein domains. B) Brain MRI scan obtained at 2 weeks revealed severely diminished cerebellar and pontine size with otherwise normal formation of cortical gyri; sagittal, coronal, and transverse planes can be seen from left to right, respectively. C) Power spectral density curves in the 0.01–50Hz range for each electrode independently; colors correspond to underlying cortical location of a given electrode. D) Quantification of mean power spectral density for each electrode in the entire 0.01–50Hz range. E) Mean power spectral density divided into biologically relevant frequency bands of delta, theta, alpha, beta, and low gamma divided by lobe; error bars represent standard deviation between electrodes within a given lobe. F) Example of a burst suppression pattern observed in the R27Ter EEG trace. Red box indicates the onset and duration of the burst suppression.

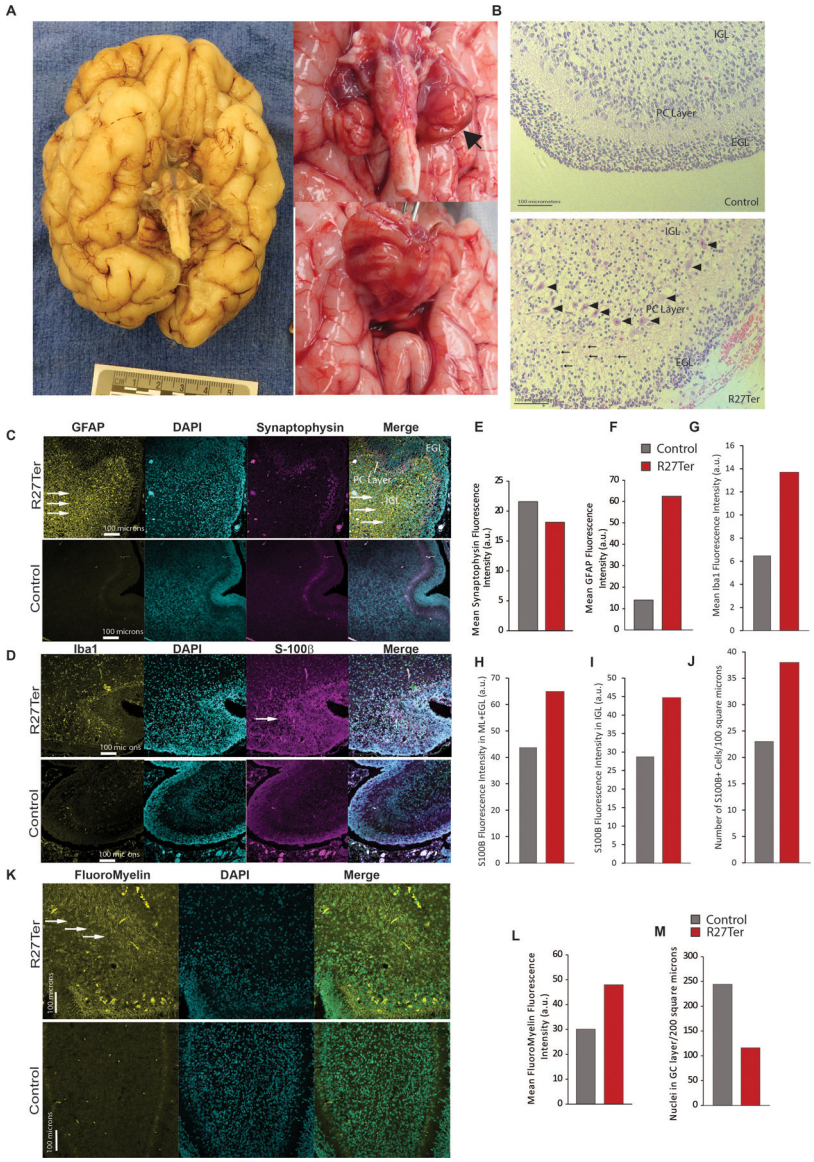

Figure 2. Absence of CASK leads to smaller brain with normal gyrification and cellular migration but increase in gliosis within cerebellum.

A) Gross image of the underside of the brain of the decedent showing normal gyri development with a severely diminished cerebellar volume. Proper neuronal migration is absolutely crucial for normal gyrification of cortex and appearance of the tertiary gyri as seen here. The cerebral hemispheres can be seen but the cerebellum is a thin leaf-like structure with a very rudimentary vermis (more details in Supplemental Figure 6, 7 and 8). B) H&E staining of the cerebellar cortex of a control (6 postnatal week (PNW)) female (died of unrelated cause on same day) and the R27Ter subject (10 PNW); the R27Ter mutation cerebellum exhibits proper lamination of the cerebellar cortex, with an external granular layer (EGL), internal granular layer (IGL), and Purkinje cell layer; arrowheads indicate properly aligned Purkinje cells. Compared to the 6 PNW normal cerebellum, the Purkinje cells in R27Ter cerebellum are already more developed with abundant cytoplasm and intricate dendritic arborization. The molecular layer in the R27Ter

mutation cerebellum also exhibits a higher proportion of granule cells migrating from the EGL to the IGL (arrows), with thinning of the EGL compared to a normal 6 PNW cerebellum. However, the IGL still appears to be depleted. C) Representative images of GFAP and synaptophysin immunostaining in the R27Ter and a control human cerebellum; from left to right: GFAP, DAPI, synaptophysin, merge. Arrows indicate increased GFAP immunoreactivity. (D) Representative images of Iba1 and S100β immunostaining in control and R27Ter subjects, showing increased Iba1 immunoreactivity in the R27Ter cerebellum. (E) Quantification of synaptophysin immunostaining fluorescence intensity between R27Ter and control cerebella, demonstrating that immunoreactivity for synaptophysin is unaltered in the absence of CASK. (F-I) Quantification of GFAP, S100β, and Iba1 fluorescence intensity, indicating increased immunoreactivity for GFAP, S100β, and Iba1 in the R27Ter cerebellum compared to control. (J) Quantification of S100β+ cells per 100 μm^2 in the R27Ter and control cerebella; a 100 μm^2 window, including the IGL and Purkinje cell layers, was used for quantification. (K) FluoroMyelin staining of R27Ter and control cerebella, indicating disorganized white matter in the R27Ter subject. (L) Quantification of FluoroMyelin fluorescence intensity. (M) Quantification of DAPI+ nuclei in the granular layer, indicating a decreased number of cells.

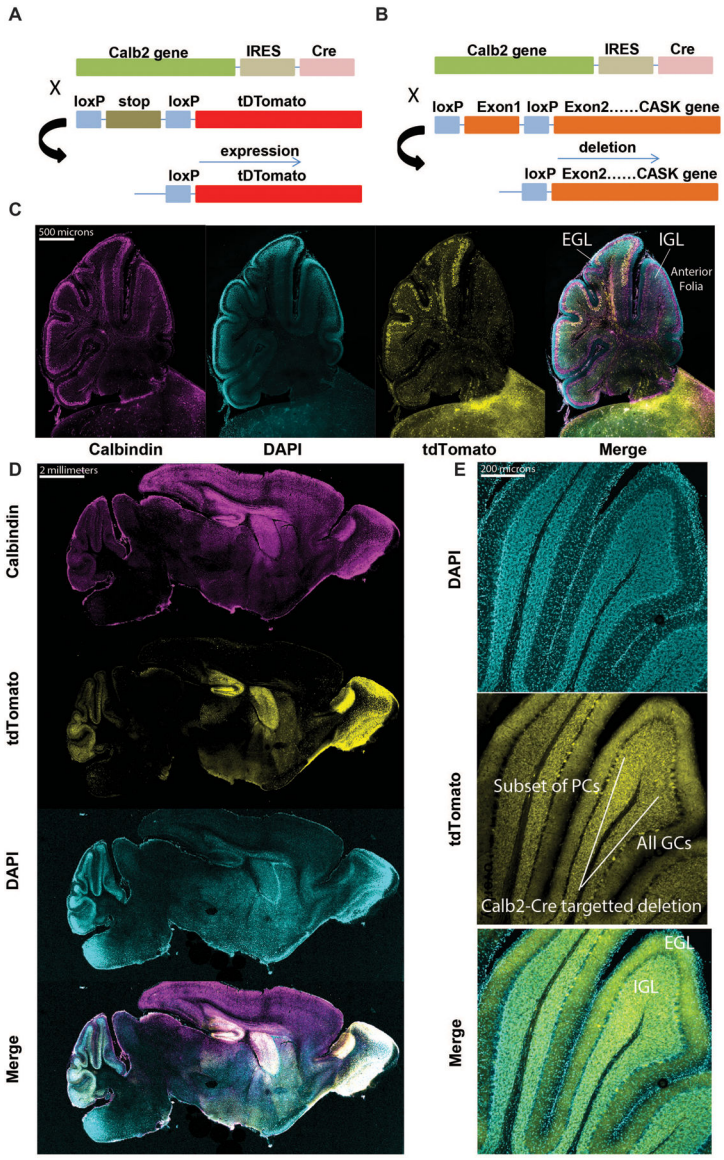

Figure 3. *Calb2*-Cre expresses only in post-migratory cerebellar granule cells and a subset of Purkinje cells in the anterior folia.

(A) Employing the LoxP-STOP-LoxP tdTomato reporter mice for determination of cell-type and age-specific Cre-mediated recombination; tdTomato expression serves as a proxy for CASK deletion in subsequent panels. (B) Schematic of breeding strategy used to selectively delete *Cask* from cerebellar cells. (C) Sagittal section of cerebellum at P8, demonstrating recombination in a subset of Purkinje cells and cells in the internal granular layer, but not in granule cells of the external granular layer; from left to right: calbindin, DAPI, tdTomato, merge. (D) 20x images of a sagittal section of whole mouse brain at P15, demonstrating recombination in several brain regions, notably the cerebellum, olfactory bulb (OB), hippocampus (Hipp.), and striatum (Str.) after development; from top to bottom: calbindin, tdTomato, DAPI, merge. (E) Higher magnification images of cerebellar folia at P15, demonstrating recombination in virtually all cells in the granular layer but only in a small subset of Purkinje cells; box indicates a sample of the subpopulation of Purkinje cells

expressing tdTomato reporter, and bracket indicates all granule cells observed expressing tdTomato. The Purkinje cell (PC) layer, molecular layer, IGL, and EGL are indicated for one folium for anatomical orientation.

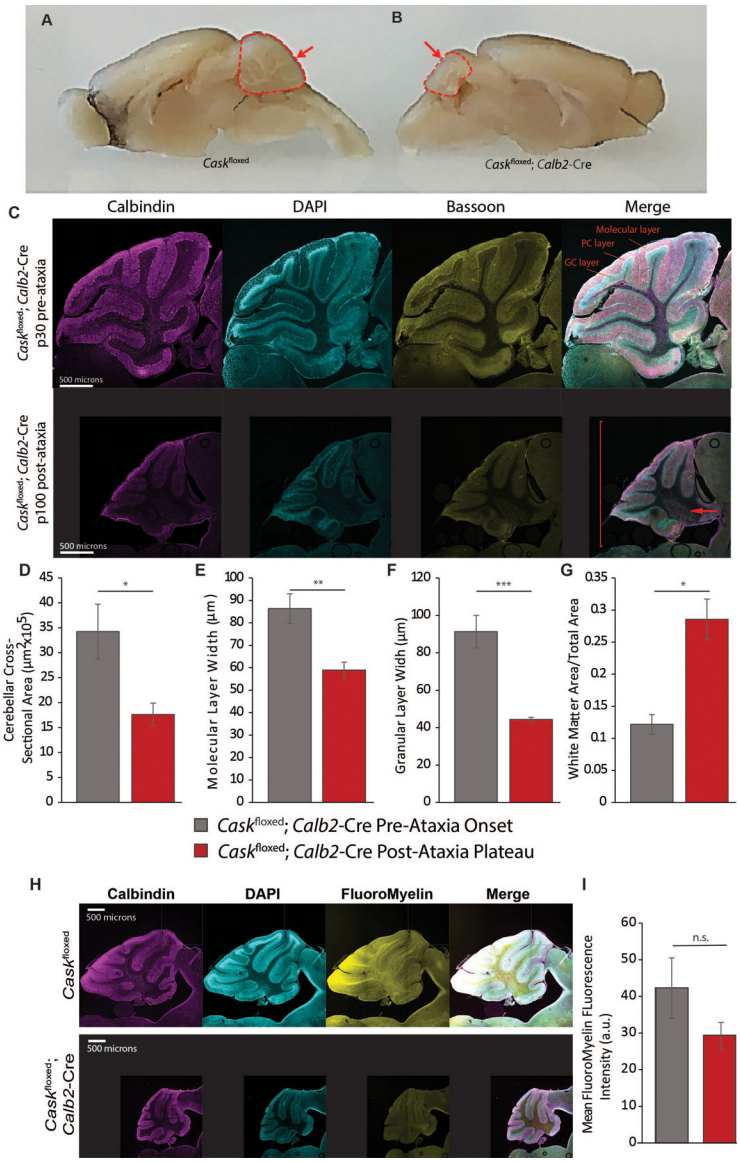

Figure 4. Deletion of *Cask* from post-migratory cerebellar cells results in profound cerebellar degeneration.

(A) Gross images of age-matched *Cask*^{floxed} control and (B) *Cask*^{floxed};*Calb2*-Cre brains after plateau of ataxia; arrow indicates diminished volume of the cerebellum while the remainder of the brain remains similarly sized. (C) 10x image of *Cask*^{floxed};*Calb2*-Cre at P30 (top) and P100 (bottom), demonstrating severely reduced cross-sectional area, molecular layer width and granular layer width at P100; the arrow indicates expanded white matter; the bracket indicates diminished overall cerebellar size. (D-F) Quantification of the entire cross-sectional area pre- and post-ataxia, molecular layer width, and granular layer width. (G) Ratio of white matter area to total cross-sectional area pre- and post-ataxia. n=3 for (B-G). (H) Cerebella of adult *Cask*^{floxed};*Calb2*-Cre post-ataxia plateau and *Cask*^{floxed} controls were labeled for calbindin, DAPI and FluoroMyelin (white matter). The mice display disorganized white matter with loss of myelinated fibers in the anterior folia.

(I) Quantification of pixel intensity of FluoroMyelin performed with n=4 mice of each genotype.

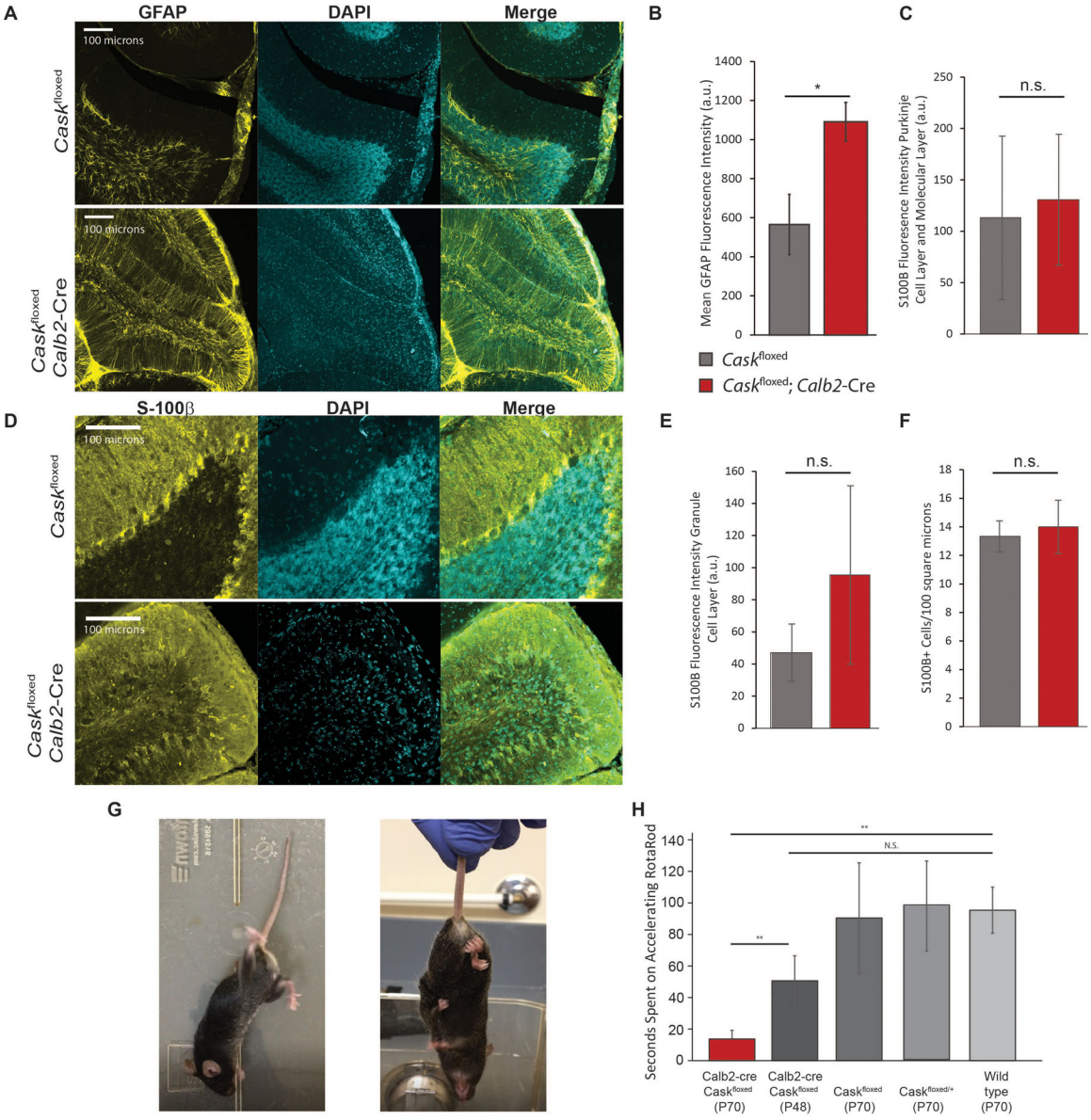

Figure 5. Reactive astrogliosis and locomotor incoordination resulting from cerebellar degeneration caused by CASK loss.

(A) Representative images of GFAP immunostaining of anterior cerebellar folia in *Cask*^{floxed};*Calb2*-Cre post-ataxia plateau and age-matched *Cask*^{floxed} controls; from left to right: GFAP, DAPI, merge. (B) Quantification of fluorescence intensity of GFAP staining by genotype; asterisk indicates $p<0.05$, n=3 mice of each genotype. (C-E) Representative images and quantification of S100β immunostaining in *Cask*^{floxed}; *Calb*-Cre compared to *Cask*^{floxed} controls. Fluorescence intensity was measured for the Purkinje cell layer and molecular layer (C) and the granule cell layer (E) separately due to the unique anatomical distribution of Bergmann glia. (F) Quantification of S100β+ cells in each genotype represented in (D). N=3 mice for each experiment; n.s. indicates $p>0.05$. (G) Example of aberrant locomotor behavior at rest (left) and hindlimb-clasping behavior in a *Cask*^{floxed};*Calb2*-Cre mouse (right). (H) Time spent on an accelerating rotarod in

seconds by genotype from left to right: *Cask*^{floxed};*Calb2*-Cre post-ataxia onset (n=4); *Cask*^{floxed};*Calb2*-Cre pre-ataxia onset (n=5); age-matched *Cask*^{floxed} controls (n=4); age-matched heterozygous *Cask*$^{floxed/+}$ controls (n=3); and age-matched wild-type controls (n=4). * indicates $p < 0.05$ using a two-tailed Student's t-test. Results are plotted as mean±SEM for all panels.

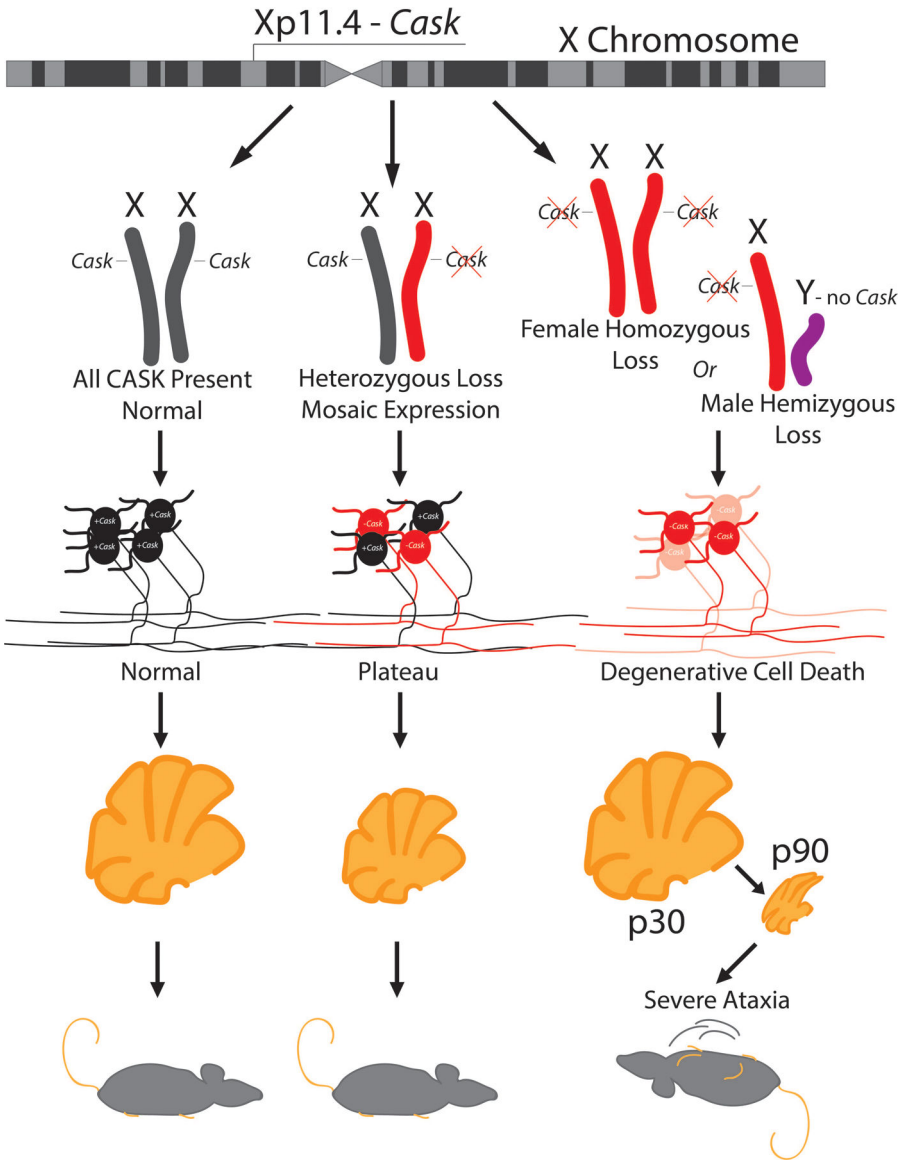

Figure 6. Model describing zygosity-based mechanism of a neurodevelopmental versus neurodegenerative clinical course of CASK-linked phenotype based on random X-chromosome inactivation.

CASK is an X-linked gene critical for maintenance of cerebellar neurons. Heterozygous mutation in CASK produces CASK loss-of-function in only 50% of neurons (red). In the heterozygous condition (red and gray), neurodegeneration thus plateaus (bottom middle), causing an apparent neurodevelopmental disorder, whereas hemizygous CASK mutations (red and purple) in male mice or homozygous CASK mutation (two reds) in female mice produce a progressive phenotype typical of neurodegeneration with severe ataxia (bottom right).